# Josephson junction simulation of neurons

Patrick Crotty,[1] Dan Schult,[2] and Ken Segall[1]
[1]*Physics & Astronomy Department, Colgate University, Hamilton, New York 13346, USA*
[2]*Mathematics Department, Colgate University, Hamilton, New York 13346, USA*
(Received 22 February 2010; revised manuscript received 25 May 2010; published 19 July 2010)

With the goal of understanding the intricate behavior and dynamics of collections of neurons, we present superconducting circuits containing Josephson junctions that model biologically realistic neurons. These "Josephson junction neurons" reproduce many characteristic behaviors of biological neurons such as action potentials, refractory periods, and firing thresholds. They can be coupled together in ways that mimic electrical and chemical synapses. Using existing fabrication technologies, large interconnected networks of Josephson junction neurons would operate fully in parallel. They would be orders of magnitude faster than both traditional computer simulations and biological neural networks. Josephson junction neurons provide a new tool for exploring long-term large-scale dynamics for networks of neurons.

DOI: 10.1103/PhysRevE.82.011914 PACS number(s): 87.19.ll, 87.19.lm, 87.19.lj

How do large networks of neurons organize, communicate, and collaborate to create the intrinsic behaviors and dynamics of the brain? Over the past century, individual neurons have been studied at the cellular, compartmental and molecular level. Synaptic models, while still somewhat rudimentary, accurately reflect many basic features of synapses and how they modify signals between neurons. Today, it is becoming feasible to explore networks of neurons behaving as units, how they synchronize, provide top-down or bottom-up feedback, and encode sensory information. This exploration is an important step toward understanding the brain, which will require multiscale analysis with models of collective behavior at many different levels simultaneously.

As part of this effort it is important that we understand how networks of neurons behave on the scale of thousands to tens of thousands of neurons, the size of a typical neocortical column. Large-scale digital simulation projects such as the Blue Brain [1,2] and PetaVision [3] projects have demonstrated that the limitations of inherently serial computer processors can be improved by effective parallel computing designs. But simulation time remains a significant hurdle to including biologically realistic features in large-scale simulations. Analog simulations using very-large-scale-integrated (VLSI) circuitry to mimic neurons and synapses are improving in realism and speed, but they are still limited by complexity and power consumption. We propose an alternate direction for analog simulation of large-scale networks of biologically realistic neurons. Using superconducting Josephson junctions to model neurons connected with real-time synaptic circuitry, we can explore neural network dynamics orders of magnitude faster than current digital or analog techniques allow. Using these circuits, we hope to learn about neural interactions such as synchronization, long term dynamics and bifurcations, feature identification, and information processing. The long term goal is to understand group behavior of neurons sufficiently to use them as building blocks for studying larger scale neural networks and brain behavior.

Our basic circuit unit (the JJ Neuron) involves two Josephson junctions connected in a loop as shown on the left side of Fig. 1. The individual junctions behave phenomenologically like ion channels: one corresponds to a depolarizing current (such as $Na^+$), and the other to a hyperpolarizing current (such as $K^+$). Enhancements are possible, of course, and the inclusion of a third junction could allow for behaviors such as bursting that generally require at least three currents. The circuit displays many features of biologically realistic neurons such as the evocation of action potentials (firing) in response to input currents or pulses, input strength thresholds below which no action potential is evoked, and refractory periods after firing during which it is difficult to initiate another action potential [4,5].

The JJ Neuron is a variation of well developed rapid single flux quantum (RSFQ) [6–8] circuitry and is thus straightforward to fabricate. RSFQ circuits using 20 000 junctions have been fabricated [9], so we estimate that a single chip could model as many as $N=10\,000$ neurons, about the number of neurons in a cortical column. For larger brain regions, chips could be connected together. A simulated action potential takes about 50 ps, and all neurons act in parallel. Table I shows a comparison of the speed of a JJ neuron with that of biological neurons and digital simulations using established models. The figure of merit displayed is the number of action potentials per neuron per second. Speed depends on the arithmetic complexity of the model employed, the number $N$ of neurons simulated and their connectivity. We show speeds for sparse (no connections between neurons) and dense (all neurons connected to all oth-

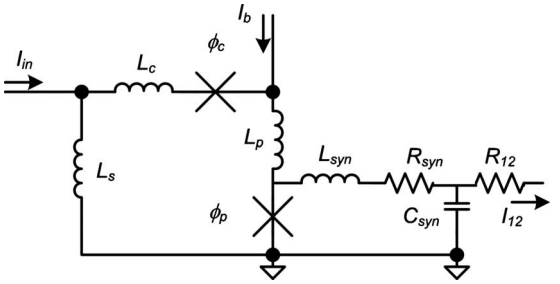


FIG. 1. Circuit diagram for the JJ Neuron (left loop) connected to a model chemical synapse (right loop). In general, many synapses could connect to a single JJ Neuron. Orientation of junction phases is chosen for clockwise current in the left loop.

 

TABLE I. Approximate number of action potentials (APs) per neuron per second for digital simulations, mammalian experiments, and the JJ Neuron. FLOPs/AP is an estimate of the floating point operations required for one AP in each digital model [4], and we assume a conservative 2 FLOPs per connection. We assume a CPU speed of $10^9$ FLOPs/second for the digital simulations. The right three columns describe the speed of a network with $N$ neurons. Sparse and dense connectivity represent extreme estimates of the computational time due to connections between neurons. Connections have no speed impact on experimental and JJ Neuron models as they are naturally parallel.

| | | AP/(neuron/s) | | |
|---|---|---|---|---|
| Model | FLOPS/AP | $N=1$ | $N=1000$ (sparse) | $N=1000$ (dense) |
| Integrate and Fire | 5 | $2.0\times10^8$ | $2.0\times10^5$ | $5.0\times10^2$ |
| FitzHugh-Nagumo | 72 | $1.4\times10^7$ | $1.4\times10^4$ | $4.8\times10^2$ |
| Izhikevich | 13 | $7.7\times10^7$ | $7.7\times10^4$ | $5.0\times10^2$ |
| Hindmarsh-Rose | 120 | $8.3\times10^6$ | $8.3\times10^3$ | $4.7\times10^2$ |
| Hodgkin-Huxley | 1200 | $8.3\times10^5$ | $8.3\times10^2$ | $3.1\times10^2$ |
| Mammalian CNS | | $1.0\times10^3$ | $1.0\times10^3$ | $1.0\times10^3$ |
| JJ Neuron | | $2.0\times10^{10}$ | $2.0\times10^{10}$ | $2.0\times10^{10}$ |

ers) networks as two extremes. While our estimates of speed are crude, they suggest that JJ Neurons are several orders of magnitude faster than either digital simulations or biological systems. This speed is due to three advantages: (a) Josephson junctions have a shorter characteristic time than the conventional transistors used in computer processors; (b) the JJ Neuron takes fewer cycles to simulate an action potential than digital simulations; and (c) JJ Neurons compute in parallel using analog connections that do not affect computation time.

This simple circuit simulates a single-compartment (space clamped) neuron and follows the spirit of mathematical neuron models such as Hodgkin and Huxley [10], FitzHugh-Nagumo [11,12], Morris-Lecar [13], Hindmarsh-Rose [14] and Izhikevich [4]. Each of these models describes the membrane potential (voltage) of the neuron as it varies in time. They also model, to varying degrees of detail, the ion channels which control the voltage via the flow of ions across the membrane. The ion channels open and close depending on the voltage thus providing the nonlinear feedback characteristic of neurons. Models differ in how many ion channels are described and their dynamic complexity. As with many of these mathematical models, our intent is not to model ion channel dynamics or chemical reactions in detail but rather to provide basic biological realism which allows us to explore the impact of network topology and connectivity strength.

The JJ Neuron attempts to mimic important neuronal behaviors: action potentials, firing thresholds and refractory periods. The primary identifying feature of a neuron is the action potential (AP), i.e., a spike or pulse in voltage across the neuron membrane as the neuron "fires." AP firing rates and interspike interval distributions are used to encode information in the brain [15]. APs require at least two independent dynamic variables, generally two voltage-gated ionic currents such as $Na^+$ and $K^+$. The inward $Na^+$ current produces the rising phase of the pulse, while the outward $K^+$ current restores the membrane to its resting potential [16]. These currents have different time scales, resulting in the characteristic shape of the action potential. The dynamics of biological voltage-gated ionic currents are complex, and subsequent models have substantially expanded on those originally proposed by Hodgkin and Huxley [17,18]. The JJ Neuron, like most neuron models, simplifies the voltage dependence of ionic currents, modeling them by junctions whose dynamics are governed by familiar second order differential equations. It does include two ionic channels and supports APs. Other important features of a neuron model include the firing threshold and refractory period. The firing threshold is a level of external stimulus below which the response is negligible, while above it an AP is triggered. The refractory period is the period of time after triggering an AP during which it is difficult to evoke a second one. Biophysically, the refractory period is determined by the time it takes the ion channel proteins to "reset" to their initial configurations. Though there are many different precise definitions of how to measure the refractory period, the important characteristic for a spatially homogeneous neuron model is an upper limit on the frequency of repeated firing.

## I. SINGLE NEURON MODEL

Josephson junctions consist of two superconductors separated by a thin insulating barrier [19]. Electrons in each superconductor are described by a coherent wave-function with a definite phase. The phase difference from one side of the barrier to the other is the so-called Josephson phase $\phi$, which controls all of the electrical properties of the junction, including the junction's voltage and current. Current can flow through the device without creating a voltage. This so-called supercurrent can be increased to the junction's critical current $I_0$ above which a voltage develops given by $V=(\Phi_0/2\pi)d\phi/dt$, where $t$ is time, $\Phi_0=h/e$ is the flux quantum, $h$ is Planck's constant and $e$ is the electron charge. Normalizing current to this critical current, the current through a junction $i$ depends on the phase $\phi$ through the relation [20]:

$$i = \ddot{\phi} + \Gamma\dot{\phi} + \sin(\phi). \quad (1)$$

The dot notation refers to differentiation with respect to normalized time $\tau$, where $\tau^2 = t^2\Phi_0 C/2\pi I_0$, with $C$ the capacitance of the junction. The normalized damping parameter is $\Gamma^2 = \Phi_0/2\pi I_0 R^2 C$, where $R$ is the resistance of the junction. The critical current, conductance $(1/R)$ and capacitance of a junction are assumed to scale linearly with the cross-sectional area $(A)$ of the junction.

Equation (1) displays a useful analogy between the dynamics of a junction and that of a pendulum, allowing us to describe the action potential-like pulse generated by the circuit. Equation (1) is exactly the equation of motion for a damped and driven pendulum, where $\phi$ represents the angle of deflection, $\Gamma$ is the normalized drag constant, and $i$ represents a driving torque. If $i$ is constant in time, long term solutions include both static tilting (gravity balancing the torque) and whirling modes (where the torque overcomes gravitational forces). A third motion is also possible that combines these two. For appropriate parameters, and time dependent torque $i$, the pendulum will whirl over just once and settle back to a tilted state. In a Josephson junction, the phase whirling over just once creates a magnetic flux pulse, called a single-flux-quantum pulse (SFQ pulse) [6]. This pulse has a similar shape and area each time it is stimulated. Pulses of this type form the action potentials in our neuron model.

The JJ Neuron circuit shown in Fig. 1 connects two Josephson junctions in a superconducting loop. This basic structure is a simplified superconducting digital component from RSFQ logic circuitry called a "dc-to-SFQ converter" [7]. We call the two junctions the pulse junction and the control junction, denoted by subscripts $p$ and $c$, respectively. Two incoming currents (normalized to $I_{0p}$) are called the input current $i_{in}$ and the bias current $i_b$ which provides energy to the circuit. The signal to the synapse is the voltage across the pulse junction $v_p = \dot{\phi}_p$, though the magnetic flux through the loop could be used for an inductive synapse circuit. The figure shows a model synaptic circuit connected above the pulse junction and thus driven by $v_p$. The circuit parameters are the indicated branch inductances $L_s$, $L_p$, and $L_c$ which we scale by their sum $L_{total}$ to obtain $\Lambda_s$, $\Lambda_p$, and $\Lambda_c$. Using current conservation and fluxoid quantization [20], we obtain two equations of motion,

$$\ddot{\phi}_p + \Gamma\dot{\phi}_p + \sin(\phi_p) = i_p = -\lambda(\phi_c + \phi_p) + \Lambda_s i_{in} + (1 - \Lambda_p) i_b, \quad (2)$$

$$\eta[\ddot{\phi}_c + \Gamma\dot{\phi}_c + \sin(\phi_c)] = i_c = -\lambda(\phi_c + \phi_p) + \Lambda_s i_{in} - \Lambda_p i_b. \quad (3)$$

with coupling parameter $\lambda = \Phi_0/2\pi L_{total} I_{0p}$, and geometric parameter $\eta = A_c/A_p$. To make the comparison with RSFQ circuitry more clear, dc-to-SFQ converters usually have $\Lambda_s \approx 1$, $\Lambda_p = \Lambda_c = 0$ and $\eta < 1$, whereas typical parameters for a JJ Neuron are $\Lambda_c = 0$, $\Lambda_s = \Lambda_p = 0.5$, and $\eta = 1$.

To explain how the circuit provides an action potential and then recharges to become ready to provide another, we describe the mechanism for generating a typical pulse. In equilibrium with $i_{in} = 0$, the bias current splits between pulse and control junctions and is large enough to put each junction just below its critical current. They are primed to achieve a whirling state. For $i_{in} > 0$, the input current acts to push the control junction away from whirling while pushing the pulse junction toward the whirling state. When the input current exceeds a threshold, it initiates the action potential: A voltage appears across the pulse junction creating magnetic flux in the loop which is analogous to a neuron's membrane potential rising. The flux in turn induces current in the loop pushing the control junction closer to its whirling state. As the flux builds, the control junction starts to whirl, draining the flux in the loop, ensuring that the pulse junction stops whirling and restoring the system so it can fire again. This process can repeat so long as the incoming current is held above threshold levels. The time lag between the pulse junction whirling, flux building and control junction responding to that flux is what creates the refractory period during which it is extremely difficult to initiate another pulse. The analogy goes beyond the membrane potential's relation to the flux $\Phi = \lambda(\phi_p + \phi_c)$ normalized by $L_{total} I_{0p}$. The pulse voltage $v_p$ is analogous to a polarizing ionic current such as $Na^+$ while the control voltage $v_c$ is analogous to a hyperpolarizing ionic current such as $K^+$.

The flux $\Phi$ in the JJ Neuron corresponds to the neuron membrane potential $V_m$. Voltages across the pulse junction, $v_p$, and control junction, $v_c$, correspond to the $Na^+$ current $I_{Na}$ and $K^+$ current $I_K$, respectively. The input current $i_{in}$ corresponds to incoming postsynaptic current $I_{syn}$. With these correspondences, the equation relating change in membrane potential to ionic currents can be written for the JJ Neuron

$$\frac{1}{\lambda}\dot{\Phi} = v_p + v_c. \quad (4)$$

The analogous equation for a neuron is the equation for a space-clamped two-channel neuron [16],

$$C\dot{V}_m = I_K + I_{Na} + I_{syn}. \quad (5)$$

The equations differ in that the synaptic current in Eq. (5), $I_{syn}$, does not appear analogously as $i_{in}$ in Eq. (4). Synaptic current does, however, appear implicitly since the phases $\phi_p$ and $\phi_c$ depend on $i_{in}$ through Eqs. (2) and (3). The results of simulations below suggest that these terms have qualitatively similar effects. Like biological APs, the JJ Neuron AP is produced by the interaction of activating and restoring processes.

## II. SINGLE NEURON CHARACTERISTICS

Single-neuron characteristics include the action potential, firing threshold and refractory period. JJ Neurons reproduce all three of these behaviors. Figure 2 shows the voltage trace and ionic currents for APs in the JJ Neuron and Hodgkin-Huxley models.

Figure 3 demonstrates the firing threshold. It shows the response to a brief current pulse of increasing strength along with an inset showing the threshold dependence of voltage peak on stimulus strength. Stimuli below threshold evoke a

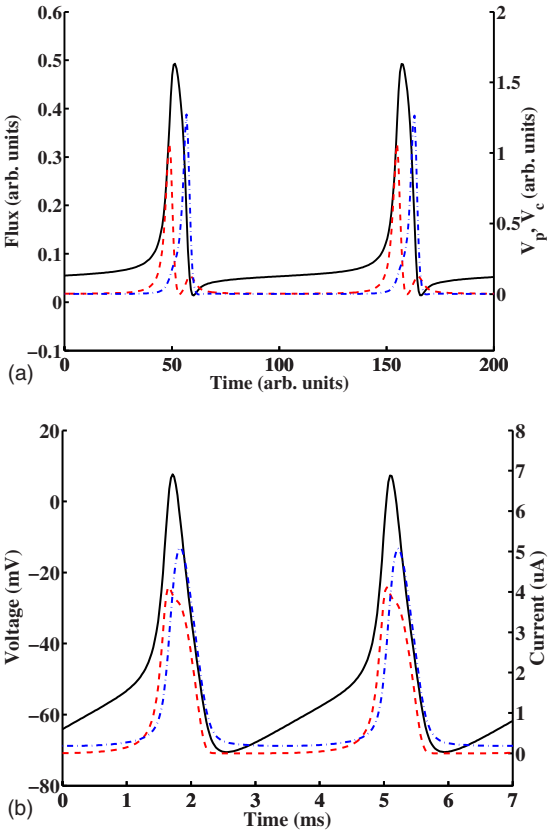


FIG. 2. (Color online) (a) Time profile for action potentials in the JJ Neuron model. Parameter values for JJ Neuron calculations are $\lambda=0.1$, $\Gamma=1.5$, $\Lambda_s=\Lambda_b=0.5$, $\eta=1$. Input dc current is $i_{in}=0.21$. (b) Time profile for action potentials in the Hodgkin-Huxley model. The flux (black solid) in the JJ Neuron corresponds to the membrane potential (black solid) in the Hodgkin-Huxley model. Similarly, the voltages $v_p$ (red dashed) and $-v_c$ (blue dot-dashed) in the JJ Neuron model correspond to the currents $-I_{\mathrm{Na}}$ (red dashed) and $I_{\mathrm{K}}$ (blue dot-dashed) in Hodgkin-Huxley model. Parameter values for all Hodgkin-Huxley calculations are $C_m=1.01$ $\mu$F/cm$^2$; $\bar{G}_{\mathrm{Na}}=120$ mS/cm$^2$; $\bar{G}_{\mathrm{K}}=36$ mS/cm$^2$; $G_L=0.3$ mS/cm$^2$; $E_{\mathrm{Na}}=50$ mV; $E_{\mathrm{K}}=-77$ mV; $E_L=-54.4$ mV; and $T=18.5$ °C unless stated otherwise. In this simulation an external stimulating current of 236 nA is applied. The Hodgkin-Huxley neurons are modeled as isopotential cylinders with lengths and diameters of 500 $\mu$m.

small (subthreshold) response, while above the threshold full APs occur.

Response to dc input is also revealing. Sufficiently large input induces repetitive spiking. The frequency of repetitive spiking at onset determines the Hodgkin class [23,24] of the neuron model. Class 1 neurons have infinite period at onset and the frequency increases with input strength. Class 2 neurons have a well defined spike frequency largely independent of the input strength. The JJ Neuron is class 2 for $\Gamma<1$ and class 1 for $\Gamma>1$. While a full bifurcation analysis is beyond the scope of this paper, this behavior reflects the bifurcation structure of a single junction with increasing current. The single junction for $\Gamma>1$ leads to an infinite period bifurcation while for $\Gamma<1$ there is a bistable region ending in a saddle node bifurcation which causes the quiescent state to jump to an oscillating solution with established frequency

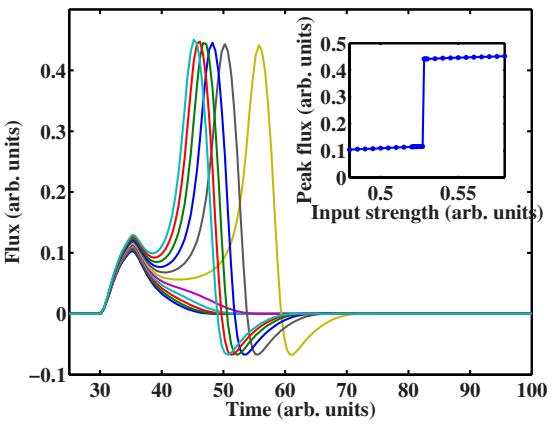


FIG. 3. (Color online) The threshold response of flux time-traces as the strength of impulse input signals increases. Stronger inputs (initially higher curves) lead to action potentials. The inset graph shows how peak response depends on the strength of the input pulse. Parameter values as for Fig. 2(a) except $\Gamma=1.0$. Input current is a single square pulse of width 5 and varied height initiated at $t=30$.

[25]. Figure 4 shows the frequency response to increasing input using a slowly ramped input current. The slow ramp effectively acts as a dc input on short time scales so the progression from quiescence to repetitive spiking is clear. For $\Gamma=0.9$ the frequency is independent of input strength (class 2) while for $\Gamma=1.5$ the frequency is zero at onset and increases with input strength (class 1).

Figure 5 demonstrates the refractory period of the JJ Neuron. Refractory period has many different precise definitions in the literature. In addition to the distinction between relative refractory period (when a super threshold current

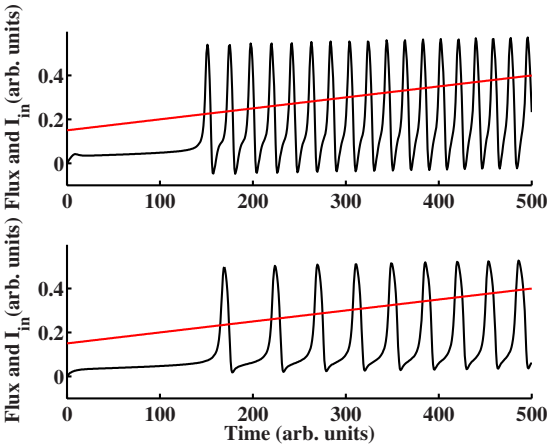


FIG. 4. (Color online) Frequency response to increased input strength. The input current (red linear) and flux response (black oscillating) curves show the frequency response due to a slow linear increase in input strength. Parameters values are as in Fig. 3 except for $\Gamma$. The top plot ($\Gamma=0.9$) shows frequency largely independent of input strength after onset of repetitive spiking. The bottom plot ($\Gamma=1.5$) shows a low frequency at onset which increases as the input strength in increased. This demonstrates that the JJ Neuron can model either class 1 or class 2 neurons depending on parameter values.

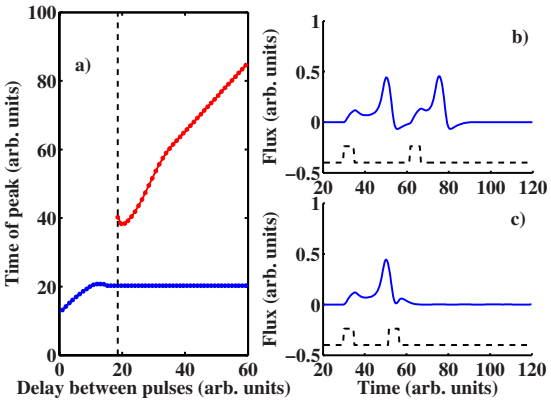


FIG. 5. (Color online) (a) Response to twin pulse inputs with delay shows the refractory period. On the left, the time of the first (lower blue) and second (upper red) response peak is graphed against the delay between input pulses. The vertical dashed line represents the delay below which no second pulse is created. On the right, time profiles are shown for input currents (green dashed) and output voltages (blue solid). In (b) two pulses are generated while in (c), the delay is too small and no second pulse arises. Parameter values as for Fig. 2(a) except $\Gamma=1.0$. Input pulses are twin square pulses of height 0.54, width 5 and varied delay between pulses. The first pulse initiates at $t=30$.

strength is needed to induce firing) and absolute refractory period (when only an extremely large stimulation will induce firing), some definitions specify it as a period of time after firing and others as a period of time after reaching threshold. One universal notion about the refractory period is that it has two major impacts on the neuron [21]. First it ensures that propagation only proceeds in one direction at a time in the axon. Our spatially homogeneous model does not address this aspect. Second the refractory period provides an upper limit on the frequency of a neuron's response. We demonstrate existence of the refractory period without choice of specific definition by showing response time to two brief current stimulus pulses as the time between pulses varies. This verifies an upper limit to the frequency of firing. Current stimuli which are too closely spaced fail to produce a second AP. We emphasize that this refractory period is not explicitly hard-coded into the model (as for integrate-and-fire models [22]), but appears naturally as a result of differences in the time scales of the activating and restoring processes just as for biological neurons. As with biological neurons, the refractory period of the JJ Neuron strongly depends on parameter values. For large delay between pulses, the firing time of the second AP depends linearly on delay. When the delay is sufficiently short, no second AP occurs. The slight upturn in the curve for the second peak corresponds to interference between two closely spaced action potentials. Plots on the right show time profiles of APs responding to two brief current pulses. The top plot shows two response APs while the bottom has only a single AP response. The maximal frequency of response can also be measured by presenting a dc input current (repeated pulse inputs with no delay) and a frequency of 0.05 is found agreeing with the refractory period of 20 shown in the figure.

## III. CONNECTING NEURONS

Synaptic models connect individual neuron models to form a network. Synapses control communication, signal transfers, and timing [26]. They can operate by means of direct electrical connections (electrical "gap junction" synapses) or chemical intermediates called neurotransmitters (chemical synapse). Electrical synapses are modeled by direct connection between JJ Neurons. We focus on chemical synapses here as they are both more complex and more common. Chemical synapses can be excitatory or inhibitory, moving the postsynaptic neuron closer to or farther from threshold, respectively. In chemical synapses, an AP causes the release of neurotransmitter molecules which diffuse across the synaptic cleft, bind to receptors on the postsynaptic membrane, and induce input currents in the postsynaptic neuron. The net effect on AP transmission across the synapse is a delay in transmission and the spreading of the pulse. We model the synaptic process using a resonant circuit attached to the pulse junction, shown on the right hand side of Fig. 1. The output is taken across the capacitor and sent through a resistor to the input of a postsynaptic neuron. If the bias current applied to the JJ neuron is positive (negative) with respect to ground, then the synapse is excitatory (inhibitory).

The equations describing our synaptic circuit and the coupling to the next neuron downstream come from Kirchhoff's laws and involve normalized parameters describing the resonant frequency $\Omega_0=\tau/\sqrt{L_{syn}C_{syn}}$, quality factor $Q=\Omega_0 R_{syn}C_{syn}/\tau$, synaptic coupling $\Lambda_{syn}=L_{syn}/L_{total}$, and resistive coupling to the next neuron, $r_{12}$, normalized by $R_{0p}$. We find that the voltage across the capacitor, $v_{out}$ (normalized by $\Gamma I_{0p}R0_p$), and the current coupled to the next neuron, $i_{12}$ (normalized by $I_{0p}$) are given by

$$\frac{1}{\Omega_0^2}\ddot{v}_{out}+\frac{Q}{\Omega_0}\dot{v}_{out}+v_{out}=v_p-\frac{Q\Omega_0\Lambda_{syn}}{\lambda}i_{12}-\frac{\Lambda_{syn}}{\lambda}\dot{i}_{12}, \quad (6)$$

$$\frac{\Lambda_{syn}(1-\Lambda_{syn})}{\lambda}\dot{i}_{12}+\frac{r_{12}}{\Gamma}i_{12}=v_{out}-\Lambda_{syn}(v_{c2}+v_{p2}). \quad (7)$$

Here $v_{p2}$ and $v_{c2}$ represent the voltage across the pulse and control junction of the next neuron, respectively.

In addition, the synapse circuit's back-action on the JJ Neuron circuit creates two additional terms on the right side of Eq. (2): $-i_{12}-\lambda v_{out}/(\Lambda_{syn}\omega_0^2)$. For the simple demonstrations of coupling behavior shown here, this back-action was not strong enough to warrant buffer junctions, as is commonly needed with RSFQ circuits [27]. However, for more complex circuits buffer junctions will most likely be needed.

We demonstrate synaptic behavior for inhibitory and excitatory coupling in a two-neuron setting. The first neuron is connected to the second via a synaptic connection as shown in Fig. 1. The results are shown in Fig. 6 and 7.

In Fig. 6, we show excitatory coupling from neuron 1 to neuron 2. Neuron 1 receives an external stimulus, and its output drives neuron 2, which responds by firing at the same rate but out of phase with neuron 1.

In Fig. 7, we show inhibitory coupling from neuron 1 to neuron 2. Neuron 2 is configured to fire repetitively by increasing its bias current. When neuron 1 is not firing, this

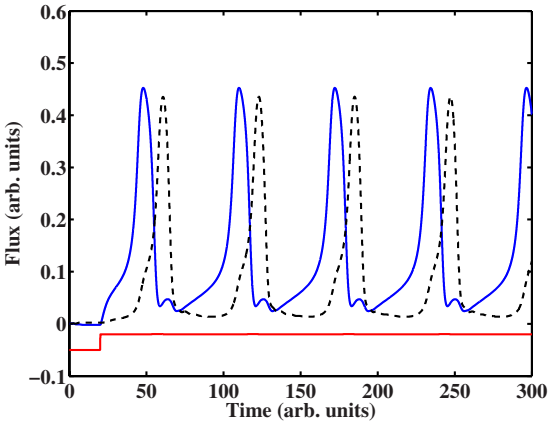


FIG. 6. (Color online) Excitatory synaptic coupling. One JJ neuron in blue (solid) drives another in black (dashed). The system is initially quiet. At time $t=20$, a constant input current (red lower) causes the first neuron to fire repetitively. Excitatory coupling induces repetitive firing of the second neuron. Parameter values as for Fig. 2(a) except $i_b=2.0$, $\Gamma=2.0$. Synaptic parameters are $\Omega=1.0$, $Q=0.05$, $\Lambda_{syn}=0.3$, $r_{12}=1.4$. Input current to first neuron is a dc current of $i_{in}=0.3$ initiated at $t=20$.

external stimulus causes neuron 2 to fire repeatedly. However, when neuron 1 is stimulated, it inhibits the firing of neuron 2 even though neuron 2 continues to receive the external stimulus. Both return to their original state after the stimulus to neuron 1 is removed. Qualitatively similar results (Figs. 8 and 9) are obtained with two coupled Hodgkin-Huxley neurons. The back-action of neuron 2 on neuron 1 causes small subthreshold oscillations and a slight decrease in the firing rate of the first neuron ($\sim 10\%$). These minor effects are not present in the Hodgkin-Huxley model because

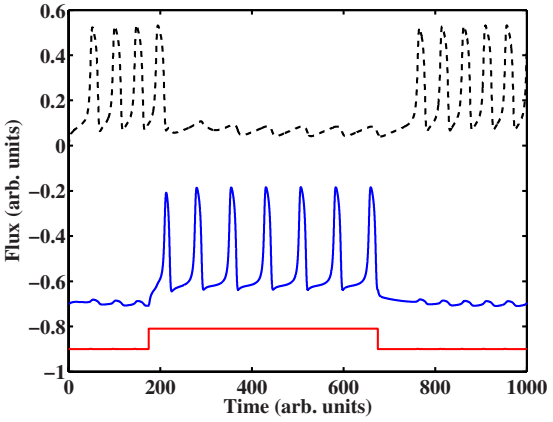


FIG. 7. (Color online) Inhibitory synaptic coupling. The second neuron (upper dashed) is configured to fire repetitively. When the first neuron (middle blue) is activated by an external input current (lower red), it inhibits the second. Both return to their original state after the external stimulus to the first neuron is removed. Parameter values as for Fig. 6 except $i_{b1}=-1.9$, $i_{b2}=1.76$, $\Lambda_{s2}=0.65$, and $\lambda_{p2}=0.35$. This pushes the second neuron into a repetitive firing mode. Synaptic parameters are also the same except $r_{12}=0.6$. Input current to first neuron is a single square pulse of height 0.3, width 500, at $t=175$. For illustrative purposes, the first neuron's flux is shifted down by $-0.7$ in the plot.

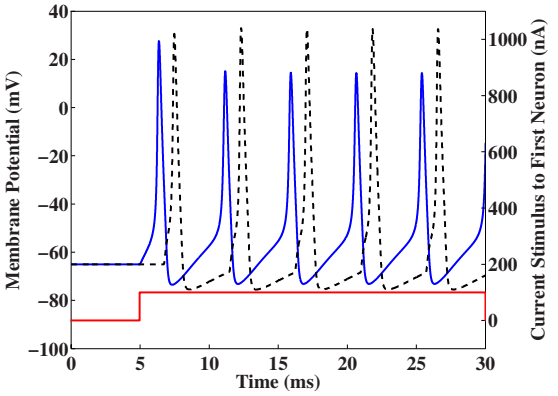


FIG. 8. (Color online) Behavior of two Hodgkin-Huxley model neurons coupled by a simple excitatory synapse model. The synapse uses a positive "alpha" function [16] with maximum current 400 nA and time scale 0.1 ms which is triggered at $-30$ mV on the downward slope of the presynaptic neuron's action potential. The presynaptic neuron in blue (solid oscillating) is made to fire repetitively by means of a constant current input (lower red curve) initiated at time 5 ms. Excitatory coupling then causes repetitive firing of the postsynaptic neuron (dashed).

the alpha function synapse does not allow back-action. Adding buffer junctions between the JJ neurons would be needed to obtain precise agreement.

## IV. DISCUSSION

We have shown that the JJ Neuron is a biologically realistic model for single neuron dynamics, and that individual JJ Neurons can be coupled together in ways that are analogous to inhibitory or excitatory chemical synaptic coupling.

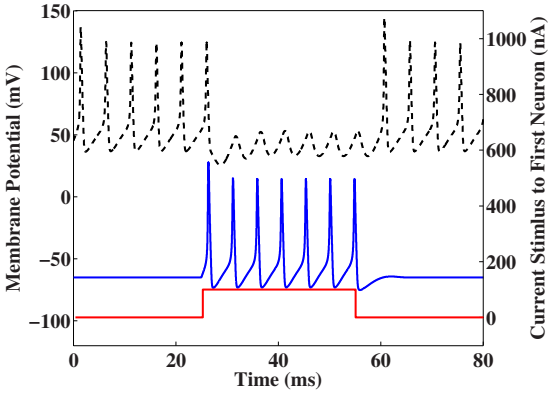


FIG. 9. (Color online) Behavior of two Hodgkin-Huxley neurons coupled with an inhibitory synapse model using a negative alpha function with maximum current 215 nA and time scale 1 ms. The second neuron (dashed) has $E_L$ set to $-15$ mV to make it fire repetitively in the absence of external inputs, while the first has $E_L$ set at the standard $-54.4$ mV value to make it normally quiescent. When the first neuron (middle blue) fires as the result of an external input current (lower red), it inhibits the second. Both return to their original state after the external stimulus to the first neuron is removed. For illustrative purposes, the second neuron's membrane potential is shifted upwards by 110 mV in the plot.

We envision that large-scale long term dynamics of networks of neurons can be explored using JJ Neurons, contributing to our understanding of behaviors such as synchronization, pattern recognition, and memory formation. JJ Neurons should be able to alleviate computational bottlenecks currently slowing needed simulations. We now discuss the advantages and limitations of this approach.

The advantages of large-scale JJ Neuron simulations are speed, biological realism, simplicity of circuit design and low power consumption. The major advantage is speed. Based on similar circuits constructed for RSFQ circuits [8], network simulations of 20 000 densely coupled neurons are reasonable and could simulate one trillion APs for each of these neurons in a few minutes. This speed is unachievable with digital simulations using modern computers. Much of this advantage is due to our analog rather than digital approach.

Analog simulations using electrical circuits to model neurons [28–33] provide a framework more in line with the parallel nature of biological neural networks. Silicon-based very-large-scale-integrated (VLSI) circuits have been designed which simulate simple integrate-and-fire neurons [34,35], bursting neurons [36], and plastic synapses with timing and homeostasis [35,37]. The focus of VLSI research has been on implementation of a learning processor rather than simulation of long-term neuron dynamics so speed comparisons are difficult. Speeds of VLSI analog circuits are typically chosen to emulate biological neuron time scales (order milliseconds). Presumably these circuit speeds could be increased up to a few gigahertz. In contrast, RSFQ processors similar to the JJ Neuron have been clocked on the order of 100 GHz [8]. In addition, the power dissipation for a JJ Neuron network should be significantly less than a VLSI circuit of the same size, allowing larger networks. Finally, the nonlinear behavior of Josephson junctions allows a JJ Neuron to contain only two Josephson junctions, much smaller than the 22 transistors for a VLSI integrate-and-fire neuron [35].

The major limitation of JJ Neuron models compared to digital simulations is measurement. While every neuron in a computer simulation can be separately monitored, this is not technically feasible in large networks of JJ Neurons. So for settings which require detailed monitoring of each cell in the network, the JJ Neuron is not appropriate. But many settings do not require such detailed observation, instead measuring averaged output or the output of a few key neurons. The measurable data from JJ Neuron experiments aligns more closely with measurements of living tissue. Placing magnetic field detectors on the chip allows measurement of averaged activity levels, and subsequent comparison of simulation data with electroencephalogram (EEG) measurements. Other settings which involve output from only a few key neurons are ripe for JJ Neuron models. Quantities such as voltage, current or flux at important points in the network can be measured directly, limited by the number of wires passing through the cooling apparatus. In addition, a variety of collective behaviors can be measured using already developed RSFQ logic circuits such as clocks, counters, splitters, followers, flip-flops, and transmission lines [7]. So, while JJ Neuron simulations are not well suited to some questions, they are for others, especially those involving averaged or collective behaviors or producing output from a small fraction of neurons. Analog simulations will not replace digital simulations. Instead, they complement each other, with analog simulations providing collective measurement on long time scales and large networks, while digital simulations provide detailed measurements on shorter time scales and smaller networks.

We are pursuing a number of potential enhancements to our JJ Neuron circuit. Along with existing tunable circuit parameters that affect the threshold, refractory period, frequency, size and shape of APs, more flexibility is possible by considering circuits with more junctions representing additional ion channels. To the extent that bursting and other exotic neuron behavior is caused by relatively slow ion channels, adding a large capacitively shunted junction (with smaller characteristic frequency) should allow JJ Neurons to display these behaviors. Plasticity of synapses based on previous history may also be possible. Connection strength can be dynamically adjusted with additional circuitry in the synapse. If the adjustments are dependent on the firing history of the neurons involved, a Hebbian learning process would be possible.

## ACKNOWLEDGMENTS

We acknowledge the generous support of Colgate University's Picker Interdisciplinary Science Institute. Special thanks to Bruce Hansen, Jason Myers, and Lyle Roelofs for helpful conversations, Jon Habif, Damhnait McHugh, Terry Orlando and Joe Amato for helpful comments, and Sarah Sciarrino for computational assistance.

[1] H. Markram, Nat. Rev. Neurosci. **7**, 153 (2006).
[2] J. G. King *et al.*, Front. Neuroinf. **3**, 10 (2009).
[3] Roadrunner supercomputer puts research at a new scale, Los Alamos National Laboratory News Release, (2008).
[4] E. M. Izhikevich, Neural Netw., IEEE Trans. **15**, 1063 (2004).
[5] F. C. Hoppensteadt and E. M. Izhikevich, *Weakly Connected Neural Networks, Applied Mathematical Sciences* (Springer-Verlag, Berlin, 1997), Vol. 126.
[6] K. Likharev and V. Semenov, IEEE Trans. Appl. Supercond. **1**, 3 (1991).
[7] P. Bunyk, K. Likharev, and D. Zinoviev, Int. J. High Speed Electron. Syst. **11**, 257 (2001).
[8] D. Brock, Int. J. High Speed Electron. Syst. **11**, 307 (2001).
[9] D. K. Brock, E. K. Track, and J. M. Rowell, IEEE Spectrum **37**, 40 (2000).
[10] A. L. Hodgkin and A. F. Huxley, J. Physiol. **117**, 500 (1952).
[11] R. A. FitzHugh, Biophys. J. **1**, 445 (1961).
[12] J. Nagumo, S. Arimoto, and S. Yoshizawa, Proc. IRE **50**, 2061

(1962).
[13] C. Morris and H. Lecar, Biophys. J. **35**, 193 (1981).
[14] J. L. Hindmarsh and R. M. Rose, Nature (London) **296**, 162 (1982).
[15] F. Rieke, D. Warland, R. de Ruyter van Steveninck, and W. Bialek, *Spikes: Exploring the Neural Code* (MIT Press, Cambridge, MA, 1999).
[16] D. Johnston and S. M.-S. Wu, *Foundations of Cellular Neurophysiology* (MIT Press, Cambridge, MA, 1995).
[17] C. A. Vandenberg and F. Bezanilla, Biophys. J. **60**, 1511 (1991).
[18] J. R. Clay, Prog. Biophys. Mol. Biol. **88**, 59 (2005).
[19] B. Josephson, Phys. Lett. **1**, 251 (1962).
[20] T. Orlando and K. Delin, *Foundations of Applied Superconductivity* (Addison-Wesley, Reading, MA, 1991).
[21] R. A. Barker and S. Barasi, *Neuroscience at a Glance* (Blackwell, Malden, MA, 2003).
[22] F. Gabbiani and C. Koch, in *Methods in Neuronal Modeling*, 2nd ed., edited by C. Koch and I. Segev (MIT Press, Cambridge, MA, 1998), Chap. 9, pp. 313–360.
[23] J. Rinzel and G. B. Ermentrout, in *Methods in Neuronal Modeling*, 1st ed., edited by C. Koch and I. Segev (MIT Press, Cambridge, MA, 1989), Chap. 5, pp. 135–170.
[24] A. L. Hodgkin, J. Physiol. **107**, 165 (1948).
[25] S. H. Strogatz, *Nonlinear Dynamics and Chaos* (Addison-Wesley, Reading, MA, 1994).
[26] *Principles of Neural Science*, 4th ed., edited by E. R. Kandel, J. H. Schwartz, and T. M. Jessell (McGraw-Hill, New York, 2000).
[27] A. M. Kadin, *Introduction to Supercomputing Circuits* (Wiley, New York, 1999).
[28] J. Keener, IEEE Trans. Syst. Man Cybern. **13**, 1010 (1983).
[29] F. Hoppensteadt, *An Introduction to the Mathematics of Neurons*, Cambridge Studies in Mathematical Biology (Cambridge University Press, Cambridge, 1997).
[30] R. Douglas and M. Mahowald, in *Methods in Neuronal Modeling* (Ref. [22]), Chap. 8, pp. 293–312.
[31] C. Bartolozzi and G. Indiveri, Neural Comput. **19**, 2581 (2007).
[32] G. Cauwenberghs and M. Bayoumi, *Learning on Silicon–Adaptive VLSI Neural Systems* (Kluwer Academic, Norwell, MA, 1999).
[33] F. Hoppensteadt, Int. J. Bifurcat. Chaos **16**, 3349 (2006).
[34] C. Mead, *Analog VLSI and Neural Systems* (Addison-Wesley, Reading, MA, 1989).
[35] G. Indiveri, E. Chicca, and R. Douglas, IEEE Trans. Neural Netw. **17**, 211 (2006).
[36] K. Hynna and K. Boahen, *Silicon Neurons that Burst when Primed*, in IEEE International Symposium on Circuits and Systems, ISCAS 2007, pp. 3363–3366 (2007).
[37] C. Bartolozzi and G. Indiveri, Neurocomputing **72**, 726 (2009).